

The H₂/O₂ Reaction on a Palladium Model Catalyst Studied with Laser-Induced Fluorescence and Microcalorimetry

Åsa Johansson*, Michael Försth and Arne Rosén

Department of Experimental Physics, School of Physics and Engineering Physics
Göteborg University and Chalmers University of Technology

SE-412 96 Göteborg, Sweden

Telephone +46 31 7723296, Facsimile +46 31 7723496

URL: <http://fy.chalmers.se/f3c> *Email: asa@fy.chalmers.se

*Author to whom correspondence should be addressed.

Received: 28 September 2001 / Accepted: 6 November 2001 / Published: 13 November 2001

Abstract: The H₂/O₂ reaction on a polycrystalline palladium foil has been studied. The experimental methods used were Laser-Induced Fluorescence (LIF) and microcalorimetry. The reaction was also simulated with the Chemkin software package. The water production maximum occurs at 40% H₂ and the OH desorption has its maximum at 10% H₂, at a total pressure of 100 mTorr (13 Pa) and a catalyst temperature of 1300 K. It is concluded, in agreement with the simulations, that the main water-forming reaction at these experimental conditions is OH+H→H₂O. From the water production maximum the quotient of the initial sticking coefficient for hydrogen and oxygen (S_{H₂}(0)/S_{O₂}(0)) is calculated to be 0.75(±0.1).

Keywords: Heterogeneous catalysis, palladium, water formation, Laser-Induced Fluorescence, sticking coefficient

Introduction

Catalysis is of great fundamental, practical and economic interest in today's society. Noble metals, such as palladium and platinum, are widely used as heterogeneous catalysts for reduction of car exhausts. The catalytic properties of platinum have been extensively studied in our group among others ([1], and references therein). We now intend to further investigate the palladium metal. The OH desorption has previously been measured with LIF [2]. New in this work is that we have used an im-

proved calibration for the gas mixture, studied the water production with microcalorimetry, and simulated the reaction by using the Chemkin software package. These experiments were done in order to determine the mechanism for water formation and to obtain information about the sticking coefficients for H₂ and O₂.

The H₂/O₂ reaction was chosen as a model system to make experiments and simulations as simple as possible, avoiding the more complex hydrocarbons. It is assumed that the oxygen and hydrogen molecules adsorb and dissociate on the surface. They react via reaction intermediates as atomic O, H, and OH to form water. The water formation rate was monitored with microcalorimetry. The hydroxyl radical OH can be conveniently studied with Laser-Induced Fluorescence. Using this technique, information can be obtained about the gas-phase concentration of OH molecules outside the catalyst. This, compared with the water formation rate, will give us essential information about the mechanism.

Water formation on palladium is discussed in several papers, for example [3, 4, 5]. In [3] a kinetic modeling of the H₂/O₂ reaction on a polycrystalline palladium surface was done. This model is of a modified Langmuir-Hinshelwood type and it takes into account the possibility that hydrogen may absorb on the interface sites. The simulations were done in the temperature range 350-475 K. The water formation on a polycrystalline palladium membrane was measured at a total pressure of 760 Torr in a hydrogen, oxygen and argon mixture [4]. The partial pressures of O₂ and H₂ were together 20% of the total pressure. The water formation was studied at 373 K, 423 K and 473 K, but it was only possible to determine the $\alpha_{\text{H}_2\text{Omax}}$, the relative hydrogen concentration at maximum water production, at 373 K because of difficulties in measuring the reactants' surface pressures. In [5] a mechanism for the water formation on a Pd(100) surface was presented, at a temperature of 215 K. The surface was studied in a UHV system with a base pressure of $1 \cdot 10^{-10}$ Torr, with high resolution angle-resolved electron energy loss spectroscopy, EELS. From the EELS spectra, the main water-forming reaction could be determined.

The palladium metal easily forms oxides that can affect the catalytic activity. The oxidation of palladium at the atomic scale is thoroughly investigated in, for example, [6]. Although oxide formation is a problem under certain operating conditions, it should not occur at the low pressures and high temperatures we are working at [7]. The palladium metal can also absorb large amounts of hydrogen, as mentioned above; see for example [8].

Methods

Laser-Induced Fluorescence was used to probe OH desorbing from the catalytic surface. The laser light was transformed into a thin sheet and a CCD array was used as detector. This made two-dimensional imaging feasible. The vacuum system consisted of a Roots-pumped (Balzers WKP 250A) stainless steel chamber. The catalyst was a polycrystalline palladium foil with purity 99.99% (Goodfellow) and had the dimensions 3.8x20x0.025 mm. Frequency-doubled light from an excimer-pumped dye laser (Lambda Physik EMG 102 E and FL 2002 E) was used to excite the OH molecules. The light from the dye laser is tunable and was scanned around $\lambda = 307$ nm, over the $X^2\Pi(v''=0) \leftarrow A^2\Sigma^+(v'=0)$ band in the OH molecule. For detection of the fluorescence signal the R₁(5) transition was used, because it has the weakest temperature dependence [9]. The catalytic foil was resistively heated to 1300 K for all experiments. The temperature was measured by a four-point resistance measurement and kept

constant with a LabVIEW-based PID-controller. The laser beam was formed into a thin sheet with two lenses forming a telescope and subsequent cylindrical optics. The fluorescence signal was imaged perpendicular to the laser sheet with a gateable ICCD camera (Princeton Instruments). The laser beam profile was also recorded as it exited the chamber, with a TE/CCD camera (Princeton Instruments) in order to normalize for intensity variations within the laser sheet. A close-up picture of the experimental set-up is shown in Fig. 1.

The hydrogen and oxygen gas flow was regulated with two mass flow controllers (Vacuum General FC6-21), one for each gas. The ratio between the partial pressures of the gases, α_{H_2} , was varied (1):

$$\alpha_{\text{H}_2} = \frac{P_{\text{H}_2}}{P_{\text{H}_2} + P_{\text{O}_2}} \quad (1)$$

The gases were mixed and the mixture entered the chamber through an orifice (diameter 20 mm) 30 mm below the palladium foil. The total mass flow was set to a constant 100 SCCM (1 SCCM = 1 Standard Cubic CentiMetre $\approx 4.08 \cdot 10^{17}$ molecules/s at $T = 300$ K which was the temperature of the gas at the inlet [9]). The final gas composition at the inlet was calibrated with a quadrupole mass spectrometer (Balzers QMG 420). The total pressure in the chamber was 100 mTorr (13.3 Pa) for all experiments, measured with a capacitance manometer (MKS 227AAG).

The calorimetric measurements were performed at 1300 K, within the same experimental set-up, by measuring the electrical power required to keep the foil at a certain temperature. Using the fact that the H_2/O_2 reaction is highly exothermic (2.5 eV/molecule formed, or 240 kJ/mole) the released chemical energy was detected as a decrease in the required power. The less power needed to keep the foil at 1300 K the more water was produced, also measured at different gas compositions, α_{H_2} . For more detailed information on the experiments, see for example [9].

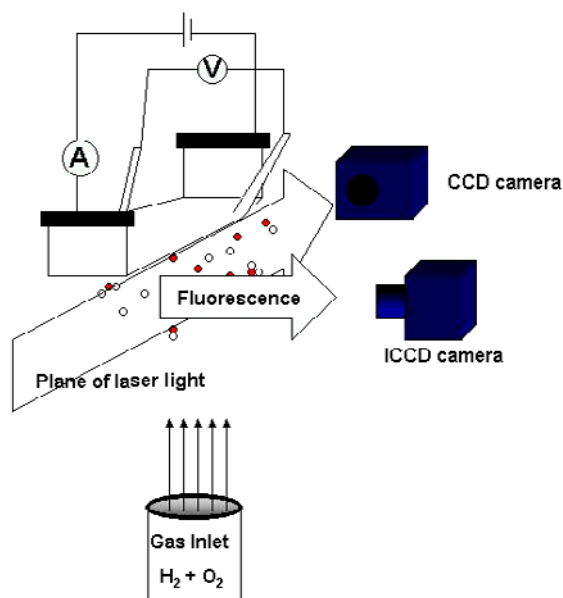


Figure 1. A close-up picture of the experimental set-up.

The Chemkin software package was used to simulate the experiment. The code Spin [10] is used to simulate the stagnation flow problem. Spin runs in conjunction with Chemkin [11] which defines the

gas-phase mechanics, Surface Chemkin [12] which defines the surface-phase mechanism, and Transport [13] which defines the transport properties. Thermodynamic data are obtained from the Thermodynamic Data Base [14]. Spin uses the Twopnt [15] solver, which implements a variant of Newton's method and a possible time evolution if the initial guess does not lead to convergence.

Results and Discussion

The experimental results are shown in Fig. 2. This figure contains useful data, which allow us to determine two interesting properties of the H_2/O_2 reaction:

- The quotient $S_{H_2}(0)/S_{O_2}(0)$ of the initial sticking coefficients for H_2 and O_2 can be calculated from the relative hydrogen pressure, α_{H_2} , where the production of water reaches a maximum: α_{H_2Omax} .
- Information about the relative importance between reaction paths S6 and S7 in Table 1 can be obtained from the positions of α_{H_2} for the maxima in the OH and H_2O curves in Fig. 2.

These considerations, which will be described below, are the basis for this study.

The maximum in OH desorption occurs at $\alpha_{H_2} = 10\%$ (α_{OHmax}), which is lower than the early results in [2], where it was measured to be $\alpha_{H_2} = 20\%$ at 100 mTorr. Ljungström and co-workers used a one-point measurement technique and their α_{H_2} values were not calibrated with a mass spectrometer. As the α_{H_2} ratio goes to zero or infinity, there should not be any OH production. However, this seems not to be the case in the oxygen-rich end, as the OH intensity has a non-zero value. According to [2], with pure oxygen, the OH molecules are formed in a reaction between oxygen and already adsorbed background water molecules – the reverse reaction S7 in Table 1, which shows the proposed reaction mechanism for the water production on Pd. The maximum in the water production was measured to be $\alpha_{H_2} = 40\%$ (α_{H_2Omax}), as also seen in Fig. 2. Both curves are normalized to unity.

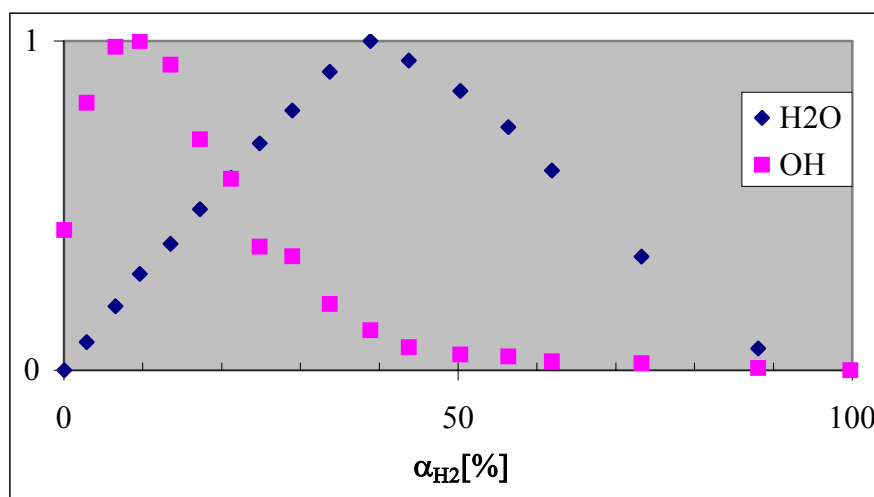


Figure 2. Normalized dependence of OH desorption and water production rates as a function of gas composition (α_{H_2}).

Ratio between initial sticking coefficients for H_2 and O_2

A very important parameter in catalysis is the initial sticking coefficient $S(0)$. It is a measure of the probability that a molecule will adsorb onto a clean surface. In the mean field approximation, the stick-

ing probability is assumed to decrease according to (2):

$$S(\theta) = S(0)(1-\theta)^i \quad (2)$$

where the degree of coverage (θ) is defined as the ratio of adsorbed molecules per surface area and adsorption sites per surface area. $S(\theta)$ is the coverage-dependent sticking coefficient (not discussed in this article), $S(0)$ is the initial sticking coefficient, and i is the order of adsorption [16]. In our simulations we have used $i=1$ for hydrogen and $i=2$ for oxygen [9].

Assuming that the maximum in water production occurs when the transport of reactants to the surface is stoichiometric, that is, with two adsorbed H_2 molecules for each O_2 molecule, we can set

$$v_{H_2}S_{H_2}(\theta)/v_{O_2}S_{O_2}(\theta) = 2 \quad (3)$$

where v is the impingement rate [17]:

$$v = p/(2\pi mk_B T)^{1/2} \quad (4)$$

For the value of α_{H_2} where maximum water production occurs, $\alpha_{H_2} = \alpha_{H_2Omax}$, the coverage is assumed to be low ($S(\theta) \approx S(0)$ in Eq. (2)). Combining this with (1), (3), and (4) gives the ratio between the hydrogen $S_{H_2}(0)$ and oxygen $S_{O_2}(0)$ initial sticking coefficients [18], valid for low coverages:

$$\frac{S_{H_2}(0)}{S_{O_2}(0)} = 0.5 * \frac{1 - \alpha_{H_2Omax}}{\alpha_{H_2Omax}} \quad (5)$$

In our case the quotient $S_{H_2}(0)/S_{O_2}(0) = 0.75$. If we estimate α_{H_2Omax} to be within $40\% \pm 3\%$, the quotient $S_{H_2}(0)/S_{O_2}(0)$ will then be 0.75 ± 0.1 . For example, according to [3], $S_{H_2}(0)/S_{O_2}(0) = 1/0.8 = 1.25$, or to [19], $S_{H_2}(0)/S_{O_2}(0) = 0.8/0.3 = 2.67$. Calculations of the absolute sticking coefficients can in principle be done. However, this is strongly sensitive to catalyst area and temperature near the surface. Since we do not know how much the backside of the catalyst (the upper side in Fig. 1) contributes to the water production, and since there is also an uncertainty in the gas temperature close to the surface, these calculations do not give meaningful information.

Our measured quotient agrees best with the sticking coefficient ratio of [3], although our results predict a somewhat lower value for $S_{H_2}(0)$ and possibly a higher value for $S_{O_2}(0)$. One reason for the difference between the ratios from our measured results and from the [3] data might be effects of mass-transport limitations in our measurements. It should also be kept in mind that Eq.(3) is only valid for low coverages, which are not necessarily the case in general. However, at $\alpha_{H_2} = \alpha_{H_2Omax}$ the total coverage is expected to be relatively low. In [4] α_{H_2} at maximum water production on a polycrystalline palladium foil was measured to be 0.2, at a higher pressure ($p_{total} = 760$ Torr) and at a lower temperature ($T = 373$ K). In the case of platinum, the α_{H_2} at maximum water production seems to vary over the pressure range; the higher the pressure, the lower the α_{H_2Omax} . Also for platinum the maximum water production decreases at higher temperatures; see for example [18, 20].

Table 1 Reaction scheme for the water-forming reaction, mainly based on [3], used in the Chemkin simulations. The values in brackets are for platinum [9]. The (s) indicates that the specie is adsorbed on the surface.

Reaction Number	Reaction	Preexponential/Sticking Coefficient	Activation Energy (J/Mol)
S1	$H_2 \rightarrow 2H(s)$	1.0 (sticking)	
S2	$2H(s) \rightarrow H_2$	$4.0 \cdot 10^{21}$	41500
S3	$O_2 \rightarrow 2O(s)$	0.8 (sticking)	
S4	$2O(s) \rightarrow O_2$	$4.0 \cdot 10^{21}$	(213000)
S5	$H(s) + O(s) \leftrightarrow OH(s)$	$4.0 \cdot 10^{21}$	79100
S6	$H(s) + OH(s) \leftrightarrow H_2O$	$4.0 \cdot 10^{21}$	59800
S7	$OH(s) + OH(s) \leftrightarrow H_2O + O(s)$	$4.0 \cdot 10^{21}$	59800
S8	$OH \rightarrow OH(s)$	1 (sticking)	
S9	$OH(s) \rightarrow OH$	$1.0 \cdot 10^{13}$	(245000)
S10	$O \rightarrow O(s)$	1 (sticking)	
S11	$O(s) \rightarrow O$	$1.0 \cdot 10^{13}$	(356000)
S12	$H \rightarrow H(s)$	1 (sticking)	
S13	$H(s) \rightarrow H$	$1.0 \cdot 10^{13}$	(249000)

Discrimination between reaction paths

From the experimental data we can conclude that the main water-forming reaction is reaction S6, $OH(s)+H(s)$, in Table 1, because the maxima in water production and in OH desorption occur at different α_{H_2} . If path S7, $OH(s)+OH(s)$, were the dominant one, the water production would have its maximum where the coverage of OH had its maximum. However, where the coverage of OH(s) has its maximum, the desorption rate of OH is also highest. Hence, if reaction S7 were dominant we would have $\alpha_{OH_{max}} = \alpha_{H_2O_{max}}$. Since this is not the case, it is believed that path S6, $H(s)+OH(s)$, is the dominant reaction, as this reaction depends not only on the OH coverage but also on the H coverage. At lower temperatures (~ 200 K) and much lower pressures, base pressure of $1 \cdot 10^{-10}$ Torr, it has been reported earlier [5] that the $OH(s)+OH(s)$ is the main water-forming reaction. In [3], however, it could not be determined which of the reactions S6 or S7 was the main water-forming reaction.

Sensitivity analysis

In the Chemkin calculations we have used the parameters in Table 1, taken from [3] and [9]. Formula (6) shows the normalized sensitivity coefficients:

$$s_{ik} = \frac{k_i}{X_k} * \frac{\partial X_k}{\partial k_i} \quad (6)$$

where k_i is the reaction rate for the i^{th} reaction and X_k is the mole fraction of species k . The sensitivity analysis tells us about the relative importance of different reactions with respect to the mole fraction X_k . Fig. 3 shows that the most inhibiting reaction as a whole for H_2O coverage on the surface,

at $\alpha_{\text{H}_2} = 10\%$, is the dissociative sticking of O_2 , reaction S3. This means that the surface is oxygen-poisoned at $\alpha < \alpha_{\text{H}_2\text{Omax}}$, that is, the higher the oxygen coverage, the lower the water production. The reason is that the sticking of H_2 , necessary for the water production, decreases as $(1-\theta)$; see Eq. (2), where θ is the coverage, which agrees with our measured data. Summarizing, it is seen that the determination of the sticking coefficients is an important step in the overall understanding of the H_2/O_2 reaction on Pd.

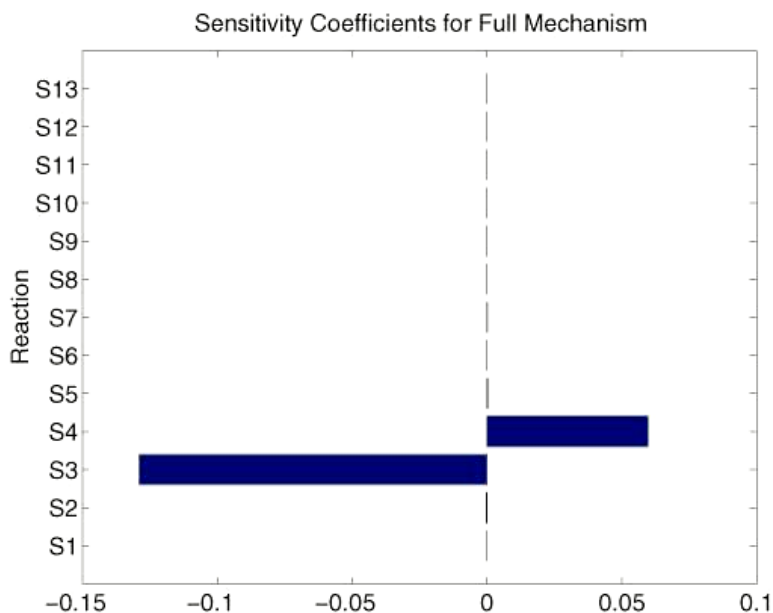


Figure 3. Sensitivity analysis with respect to surface H_2O of the reaction scheme for the H_2/O_2 reaction on Pd. The simulation was performed at $\alpha_{\text{H}_2} = 10\%$. The figure contains sensitivity coefficients for the water production on the surface. As seen, reaction S3 – dissociative sticking of O_2 – is the most important reaction, in a negative sense. This means that the surface is oxygen-poisoned. Accordingly S4, associative desorption of O_2 , is the reaction with the greatest positive sensitivity coefficient. Adsorption and desorption of intermediate species, reactions S8-S13, are unimportant for the model.

Conclusions

The mixing ratio (α_{H_2}) for maximum OH desorption was found to be about 10% (α_{OHmax}) while the maximum water production was found for $\alpha_{\text{H}_2\text{Omax}} = 40\%$. Using these values, the ratio between the hydrogen and oxygen sticking coefficients was evaluated: $S_{\text{H}_2}(0)/S_{\text{O}_2}(0) = 0.75 \pm 0.1$. The best, but not perfect, agreement in the literature for the individual sticking coefficients was found in [3]: unity for hydrogen and 0.8 for oxygen.

The fact that the water production and OH desorption maxima occur at different α_{H_2} also gives information about the relative importance of the two reaction paths S6 and S7. If reaction S7 were dominant, one would have $\alpha_{\text{OHmax}} = \alpha_{\text{H}_2\text{Omax}}$. That this is not the case leads us to believe that path S6, $\text{H}(\text{s}) + \text{OH}(\text{s})$, is the dominant one, since this reaction depends not only on the OH coverage but also on the H coverage.

Further measurements are now in progress in order to achieve a better understanding of the H₂/O₂ reaction on a palladium model catalyst at different pressures and temperatures. Generally, learning more about surface and gas-phase chemistry, and their interaction, will be of continued importance in the future.

Acknowledgement

I (ÅJ) gratefully acknowledge financial support from the Swedish Natural Science Research Council (NFR), now the Swedish Research Council (VR) (contract E-AD/EG 02560-371). MF acknowledges the Combustion Engine Research Centre, CERC, for financial support. Thanks are also due to the rest of the Molecular Physics group, especially Mats Andersson, for many fruitful discussions.

References

1. Försth, M.; Gudmundson, F.; Persson, J.; Rosén, A. *Combustion and Flame*, **1999**, *119*, 144-153.
2. Ljungström, S.; Hall, J.; Kasemo, B.; Rosén, A.; Wahnström, T. *Journal of Catalysis*, **1987**, *107*, 548-556.
3. Fogelberg, J.; Petersson, L.-G. *Surface Science*, **1996**, *350*, 91-102.
4. Johansson, M.; Ekedahl, L.-G. *Applied Surface Science*, **2001**, *173*, 122-133.
5. Nyberg, C.; Tengstål, C.G. *Journal of Chemical Physics*, **1984**, *80*(7), 3463-3468.
6. Zheng, G.; Altman, E.I. *Surface Science*, **2000**, *462*, 151-165.
7. Voogt, E.H. *Palladium Model Catalysts*. **1997**, p51, Utrecht University, Utrecht, ISBN 90-393-1752-6.
8. Sharpe, A.G. *Inorganic Chemistry*, 3rd ed., Longman Scientific & Technical, Harlow, **1992**, p224.
9. Försth, M. *Laser Diagnostics and Chemical Modeling of Combustion and Catalytic Processes*. Department of Experimental Physics, **2001**, Chalmers University of Technology and Göteborg University, Göteborg, ISSN 0346-718X.
10. Coltrin, M.E.; Kee, R.J.; Evans, G.H.; Meeks, E.; Rupley, F.M.; Grcar, J.F. *SPIN (Version 3.83): A Fortran Program for Modeling One-dimensional Rotating-Disk/Stagnation-Flow Chemical Vapor Deposition Reactors*, **1991**, Sandia National Laboratories, SAND91-8003, Albuquerque NM, Livermore CA.
11. Kee, R.J.; Rupley, F.M.; Miller, J.A. *Chemkin-II: A Fortran Chemical Kinetics Package for the Analysis of Gas Phase Chemical Kinetics*, **1989**, Sandia National Laboratories, SAND89-8009B, Albuquerque NM, Livermore CA.
12. Coltrin, M.E.; Kee, R.J.; Rupley, F.M. *SURFACE CHEMKIN (Version 4.0): A Fortran Package for Analyzing Heterogeneous Chemical Kinetics at a Solid-Surface-Gas-Phase Interface*, **1991**, Sandia National Laboratories, SAND90-8003C, Albuquerque NM, Livermore CA.
13. Kee, R.J.; Dixon-Lewis, G.; Warnatz, J.; Coltrin, M.E.; Miller, J.A. *A Fortran Computer Code Package for the Evaluation of Gas-Phase Multicomponent Transport Properties*, **1986**, Sandia National Laboratories, SAND86-8246, Albuquerque NM, Livermore CA.
14. Kee, R.J.; Rupley, F.M.; Miller, J.A. *The Chemkin Thermodynamic Data Base*, **1987**, Sandia National Laboratories, SAND87-8215B, Albuquerque NM, Livermore CA.
15. Grcar, J.F. *The Twopnt Program for Boundary Value Problems*, **1992**, Sandia National Laborato-

ries, SAND91-8230, Albuquerque NM, Livermore CA.

16. Zangwill, A. *Physics at Surfaces*, 1st ed., Cambridge University Press, Cambridge UK, **1988**.
17. Chambers, A.; Fitch, R.K.; Halliday, B.S. *Basic Vacuum Technology*, IOP Publishing Ltd, Bristol, **1989**, p14.
18. Ljungström, S.; Kasemo, B.; Rosén, A.; Wahnström, T.; Fridell, E. *Surface Science*, **1989**, *216*, 63-92.
19. Meijere, A.D.; Kolasinski, K.W.; Hasselbrink, E. *Faraday Discussions*, **1993**, *96(18)*, 1-11.
20. Elg, A-P.; Rosén, A. *Applied Physics B*, **1997**, *64*, 573-578.

© 2001 by MDPI (<http://www.mdpi.org>).